IOPscience iopscience.iop.org

Home Search Collections Journals About Contact us My IOPscience

High-power subpicosecond harmonically mode-locked Yb:YAG laser with pulse repetition rate up to 240 GHz

This content has been downloaded from IOPscience. Please scroll down to see the full text.

2013 Laser Phys. Lett. 10 015803

(http://iopscience.iop.org/1612-202X/10/1/015803)

View the table of contents for this issue, or go to the journal homepage for more

Download details:

IP Address: 140.113.38.11
This content was downloaded on 28/04/2014 at 01:08

Please note that terms and conditions apply.

Laser Phys. Lett. **10** (2013) 015803 (4pp) doi:10.1088/1612-2011/10/1/015803

LETTER

High-power subpicosecond harmonically mode-locked Yb:YAG laser with pulse repetition rate up to 240 GHz

Y F Chen, W Z Zhuang, H C Liang, G W Huang and K W Su

Department of Electrophysics, National Chiao Tung University, 1001 TA Hsueh Road, Hsinchu 30010, Taiwan

E-mail: yfchen@cc.nctu.edu.tw

Received 27 March 2012, in final form 3 July 2012
Published 7 December 2012
Online at stacks.iop.org/LPL/10/015803

Abstract
We report on the operation of a high-power diode-pumped Yb:YAG self-mode-locked microchip laser with a pulse repetition rate of up to 240 GHz. The gain medium is coated to form a cavity mirror and to act as an etalon for achieving harmonic mode locking. A diamond heat spreader is employed to reduce the thermal effects for power scale-up. At an absorbed pump power of 8.3 W, an average output power of 4.6 W is achieved with a pulse duration of 630 fs and a repetition rate of 240 GHz.

(Some figures may appear in colour only in the online journal)

Pulsed lasers with repetition rates higher than 10 GHz attract noticeable interest for applications such as in wireless communication [1], telecommunication [2], quantum communication [3], high signal-to-noise ratio measurements [4], photonic switching [5], and large-mode-spacing supercontinuum generation [6]. The methods for achieving such high-repetition-rate light sources include harmonically mode-locked fiber lasers [7, 8], quantum-well Fabry–Perot lasers [9], quantum-dash-based Fabry–Perot mode-locked lasers [10], passively harmonically mode-locked vertical-external-cavity surface-emitting lasers [11, 12], and passively mode-locked solid-state lasers [13, 14]. Among solid-state gain media, diode-pumped ytterbium (Yb) doped lasers have been identified as excellent systems for compact efficient femtosecond light sources because Yb-doped materials have small quantum defects and high quantum efficiencies. Recently, Kerr-lens mode-locking experiments have been demonstrated for the Yb-doped gain media including Yb:$KY(WO_4)_2$ [15], Yb:YVO_4 [16], Yb:Y_2O_3 [17], and Yb:YAG [18] crystals. However, so far the pulse repetition rates never exceed 1 GHz in the Kerr-lens mode-locked Yb-doped lasers. More recently, self-mode-locked operation with a linear cavity has also been observed in numerous end-pumped solid-state and semiconductor lasers [19–22]. The physical mechanism is speculated to be associated with the combined effects of the Kerr-lensing and thermal lensing [17–22]. The feasibility of compact linear cavities paves the way for the development of mode-locked lasers with ultra-high repetition rates.

In this letter we report a high-power subpicosecond harmonically mode-locked laser with sub-terahertz pulse repetitions by means of a specially coated Yb:YAG microchip in a linear Fabry–Perot cavity. The front surface of the gain medium is coated to form a cavity mirror and is bonded with a diamond heat spreader to significantly enhance the output performance. The rear surface of the Yb:YAG plate is coated not only to lead to a second pass of the pump light but also to act as an etalon for achieving harmonic mode locking. We also confirm that the diamond heat spreader can enhance the output performance of the Yb:YAG microchip laser. Experimental results reveal that when the optical length of the laser cavity is close to a commensurate ratio of the optical length of the Yb:YAG plate, the laser output displays a single-pulse harmonic mode locking. The pulse repetition rate is found to be a multiple of the free spectral range caused by the etalon effect of the Yb:YAG plate, ranging from 80 to 240 GHz. Under the absorbed pump power of 8.3 W, an average output

 © 2013 Astro Ltd Printed in the UK & the USA

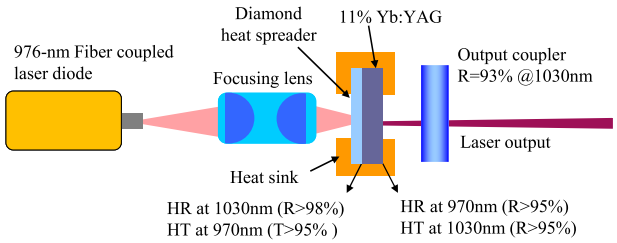

Figure 1. Schematic diagram for the experimental setup of harmonically self-mode-locked Yb:YAG lasers formed by a Fabry–Perot flat–flat cavity.

power of 4.6 W is achieved with a pulse duration of 630 fs and repetition rate of 240 GHz, corresponding to an optical efficiency of 55.4%.

Figure 1 shows the schematic diagram for the experimental setup of harmonically self-mode-locked Yb:YAG lasers formed by a Fabry–Perot flat–flat cavity. The gain medium is an 11 at.% Yb:YAG crystal with a length of 1.03 mm and a diameter of 4.0 mm. The Yb:YAG crystal is cut along the [111] direction. The front surface of the Yb:YAG plate is coated to form a cavity mirror with high transmission ($T > 95\%$) at the wavelength 970 nm of pump light and with high reflection ($R > 99.8\%$) for the lasing wavelength of 1030–1060 nm. The rear surface of the Yb:YAG crystal is coated for high reflection ($R > 95\%$) at 970 nm to lead to a second pass of the pump light and for high transmission ($T \approx 95\%$) for the lasing wavelength. The double-pass absorption of the gain medium is measured to be approximately 83%. Note that the partial reflection ($R \approx 5\%$) on the rear surface for the lasing wavelength is employed to act as an etalon for achieving harmonic mode locking.

A 4.5 mm square, 0.5 mm thick piece of uncoated single crystal diamond heat spreader was bonded to the front surface of the gain medium to improve the heat removal [23–25]. The transmittance of the diamond heat spreader is approximately 70% at 970 nm. The front surface of the diamond is in contact with a copper heat sink which is cooled by a thermal-electric cooler (TEC), where the temperature was maintained at 15 °C. The rear surface of the gain medium is attached tightly to a copper plate with a hole of 2 mm diameter, where an indium foil is employed to be the contact interface. The contact uniformity is further confirmed by inspecting the interference fringe coming from the minute gap between the gain chip and the diamond heat spreader. A flat wedged output coupler with 7% transmission at 1040 nm is used in the experiment. The pump source is a 16 W 970 nm fiber-coupled laser diode with a core diameter of 200 μm and numerical aperture of 0.20. A focusing lens with 25 mm focal length and 87% coupling efficiency is used to reimage the pump beam into the laser crystal. The average pump diameter is approximately 130 μm. Considering the coupling efficiency of the focusing lens, the transmittance of the diamond, and the effective absorption of the gain medium, the maximum available absorbed pump power is found to be 8.3 W. Note that without using the diamond heat spreader the maximum available absorbed pump power can be up to 11 W.

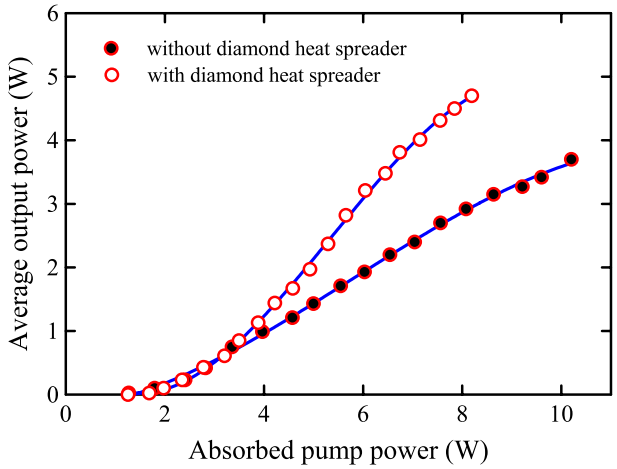

Figure 2. Output power versus absorbed pump power for the laser schemes without and with using the diamond heat spreader at a cavity length of $L_{cav} = 5.0$ mm. Note that the output characteristics are almost the same for $L_{cav} < 9.0$ mm.

First of all, we investigate the stable region of the optical cavity length L_{cav} at the maximum absorbed pump power of 8.3 W. The output power is found to be nearly the same for $L_{cav} < 9.0$ mm. On the other hand, the output power obviously starts to decrease with increasing the cavity length for $L_{cav} > 10.0$ mm because of the thermal lensing effect. Figure 2 shows the output power versus absorbed pump power for the laser schemes without and with using the diamond heat spreader at a cavity length of 5.0 mm. It can be seen that the diamond heat spreader significantly improves the slope efficiency to enhance the maximum output power up to 4.6 W. Since the diamond effectively reduces the thermal effect, the overall beam quality M^2 is found to be better than 1.3 for all the pump powers.

We exploit the schemes of first- and second-order autocorrelations to analyze the temporal behavior of the laser output. The first-order autocorrelation trace is performed with a Michelson interferometer (Advantest, Q8347) that is also capable of performing optical spectral analysis by Fourier transforming the first-order field autocorrelation. The second-order autocorrelation trace is performed with a commercial autocorrelator (APE pulse check, Angewandte Physik & Elektronik GmbH). For most cavity lengths between 4.0 and 9.0 mm, we experimentally find that the laser output displays a state of multiple-pulse mode locking with a repetition rate that is a multiple of ~80 GHz. The frequency of 80 GHz can be confirmed to come from the free spectral range of the etalon effect caused by the Yb:YAG crystal with an optical length of $L_{cry} \approx 1.87$ mm. Figures 3(a) and (b) depict the experimental traces of first- and second-order autocorrelations for the operation of a multiple-pulse mode locking obtained at a cavity length of 6.08 mm. It can be seen that the pulse separation and the temporal structure are almost the same as for the results obtained with the first- and second-order autocorrelation traces. The great resemblance between the first- and second-order autocorrelation traces implies that the phase of the optical spectrum is nearly constant [26].

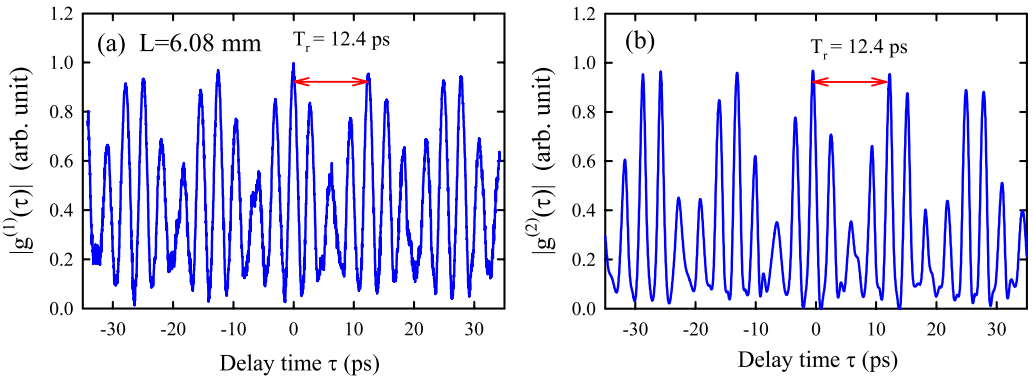

Figure 3. Experimental traces of (a) first- and (b) second-order autocorrelations for the operation of a multiple-pulse mode locking obtained at a cavity length of 6.08 mm.

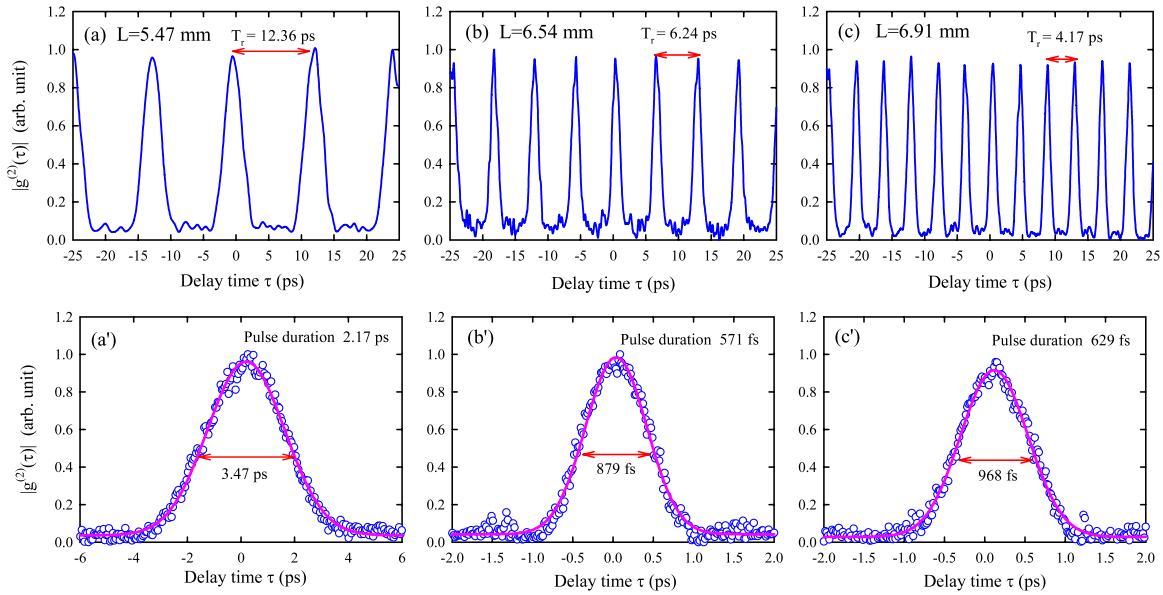

Figure 4. (a)–(c) Experimental results of the second-order autocorrelation at the maximum output power of 4.6 W for three cases of single-pulse harmonic mode locking observed at the cavity lengths of 5.47, 6.54, and 6.91 mm, respectively. (a′)–(c′) FWHM widths of the central peaks of the second-order autocorrelation shown in (a)–(c), respectively.

By scanning all the optical cavity lengths, we experimentally find that when the optical cavity length L_{cav} is adjusted to be close to a commensurate ratio of the crystal length L_{cry}, the single-pulse harmonically mode-locked operation can be achieved. Figures 4(a)–(c) show the experimental results of the second-order autocorrelation at the maximum output power of 4.6 W for three cases of single-pulse harmonic mode locking observed at the cavity lengths of 5.47, 6.54, and 6.91 mm, respectively. The pulse repetition rates can be seen to be approximately 80, 160, and 240 GHz for the operations shown in figure 4(a)–(c). The free spectral ranges of the laser cavities are 27.7, 23.1, and 21.9 GHz for the cavity lengths of 5.47, 6.54, and 6.91 mm. With these free spectral ranges, we can deduce that the operations of harmonic mode locking in figures 4(a)–(c) are third, seventh, and 11th orders, respectively. The ratios L_{cry}/L_{cav} for the cases shown in figures 4(a)–(c) are indeed quite close to the fractional numbers of 1/3, 2/7, and 3/11, respectively. Figures 4(a′)–(c′) depict the full width at half maximum (FWHM) widths of the central peaks of the second-order autocorrelation traces shown in figures 4(a)–(c), respectively. Assuming the temporal intensity to be a sech^2 profile, the pulse durations can be found to be 2.17, 0.57, and 0.63 ps for the cases shown in figure 4(a′)–(c′). To further validate the quality of harmonic mode locking, we also employ the digital oscilloscope for the real-time trace and RF power spectrum analyzer with the bandwidth limit of the instrument up to 10 GHz. We also do not observe any sign of Q-switched mode locking in either autocorrelation or the RF spectrum.

Figures 5(a)–(c) show the measured results of the first-order autocorrelation corresponding to the cases shown in figures 4(a)–(c). Similar to the result shown in figure 2, the pulse separation and the temporal structure obtained with the first-order autocorrelation traces are nearly the same as the results obtained with the second-order scheme. Figures 5(a′)–(c′) depict the optical spectra derived from the experimental first-order autocorrelation traces shown in figures 5(a)–(c), respectively. It can be seen that the numbers

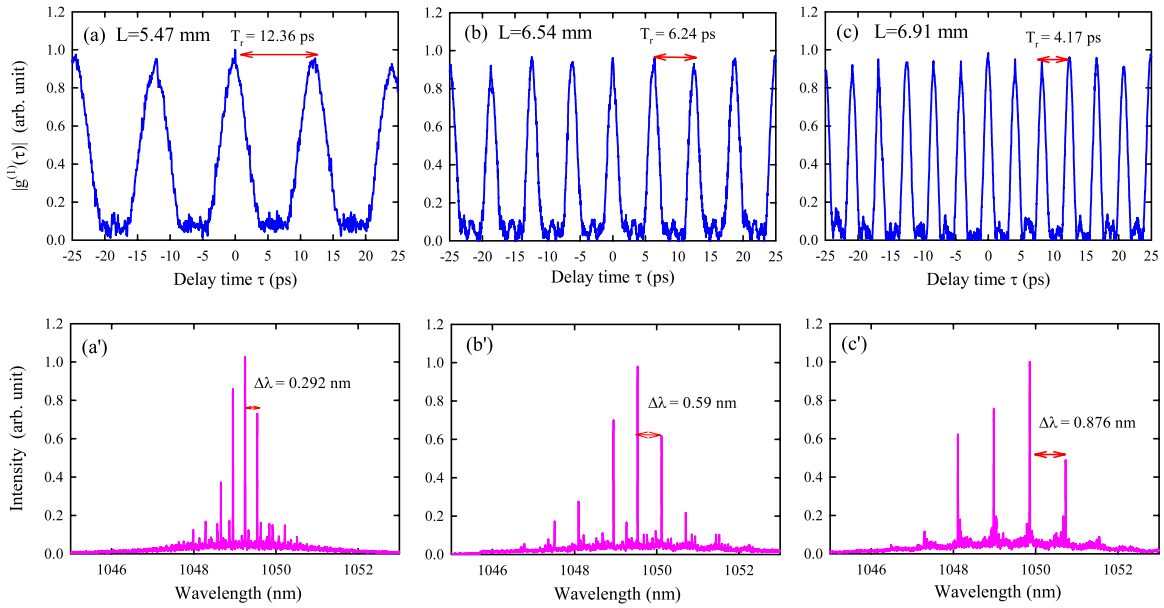

Figure 5. (a)–(c) Experimental results of the first-order autocorrelation traces corresponding to the results shown in figures 4(a)–(c), respectively. (a′)–(c′) Optical spectra corresponding to the first-order autocorrelation traces shown in (a)–(c), respectively.

of principal lasing modes are approximately four–five. The values of the mode spacing for all cases are consistent with the pulse repetition rates shown in figures 4(a)–(c).

In conclusion, we have demonstrated the experimental observation of high-power self-mode-locked operation in a diode-pumped Yb:YAG microchip laser with a pulse repetition rate of up to 240 GHz. The front surface of the gain medium is coated to form a cavity mirror and its rear surface is coated to lead to a second pass of the pump light and to act as an etalon for achieving harmonic mode locking. A diamond heat spreader is employed to reduce the thermal effects for power scale-up. It is experimentally found that the single-pulse harmonically mode-locked operation can be acquired by adjusting the optical lengths of the laser cavity to be close to a commensurate ratio of the optical length of the Yb:YAG plate. At an absorbed pump power of 8.3 W, an average output power of 4.6 W is achieved with a pulse duration of 630 fs and a repetition rate of 240 GHz.

Acknowledgments

The authors acknowledge the National Science Council of Taiwan (NSCT) for their financial support of this research under contract NSC 100-2628-M-009-001-MY3.

References

[1] Federici J and Moeller L 2010 *J. Appl. Phys.* **107** 111101
[2] Tomaru T and Petek H 2000 *Opt. Lett.* **25** 584
[3] Silberhorn Ch, Lam P K, Weiß O, König F, Korolkova N and Leuchs G 2001 *Phys. Rev. Lett.* **86** 4267
[4] Bartels A, Dekorsy T and Kurz H 1999 *Opt. Lett.* **24** 996
[5] Miller D A B 1989 *Opt. Lett.* **14** 146
[6] Bartels A, Heinecke D and Diddams S A 2009 *Science* **326** 681
[7] Yoshida E and Nakazawa M 1996 *Electron. Lett.* **32** 1370
[8] Schröder J, Coen S, Vanholsbeek F and Sylvestre T 2006 *Opt. Lett.* **31** 3489
[9] Sato K 2003 *IEEE J. Sel. Top. Quantum Electron.* **9** 1288
[10] Gosset C, Merghem K, Martinez A, Moreau G, Patriarche G, Aubin G, Ramdane A, Landreau J and Lelarge F 2006 *Appl. Phys. Lett.* **88** 241105
[11] Quarterman A H, Wilcox K G, Apostolopoulos V, Mihoubi Z, Elsmere S P, Farrer I, Ritchie D A and Tropper A C 2009 *Nature Photon.* **3** 729–31
[12] Klopp P, Griebner U, Zorn M and Weyers M 2011 *Appl. Phys. Lett.* **98** 071103
[13] Oehler A E H, Südmeyer T, Weingarten K J and Keller U 2008 *Opt. Express* **16** 21930
[14] Chen Y F, Liang H C, Tung J C, Su K W, Zhang Y Y, Zhang H J, Yu H H and Wang J Y 2012 *Opt. Lett.* **37** 461
[15] Liu H, Nees J and Mourou G 2001 *Opt. Lett.* **26** 1723
[16] Lagatsky A A *et al* 2005 *Opt. Lett.* **30** 3234
[17] Xie G Q, Tang D Y, Zhao L M, Qian L J and Ueda K 2007 *Opt. Lett.* **32** 2741
[18] Uemura S and Torizuka K 2008 *Appl. Phys. Express* **1** 012007
[19] Liang H C, Chen R C C, Huang Y J, Su K W and Chen Y F 2008 *Opt. Express* **16** 21149
[20] Liang H C, Huang Y J, Huang W C, Su K W and Chen Y F 2010 *Opt. Lett.* **35** 4
[21] Paiella R, Capasso F, Gmachl C, Sivco D L, Baillargeon J N, Hutchinson A L, Cho A Y and Liu H C 2000 *Science* **290** 1739
[22] Chen Y F, Lee Y C, Liang H C, Lin K Y, Su K W and Huang K F 2011 *Opt. Lett.* **36** 23
[23] Hopkins J M, Smith S A, Jeon C W, Sun H D, Burns D, Calvez S, Dawson M D, Jouhti T and Pessa M 2004 *Electron. Lett.* **40** 30–1
[24] Lindberg H, Strassner A, Gerster E and Larsson A 2004 *Electron. Lett.* **40** 601–2
[25] Korpijärvi V-M, Leinonen T, Puustinen J, Härkönen A and Guina M D 2010 *Opt. Express* **18** 25633–41
[26] Weiner Andrew M 2009 *Ultrafast Optics* (Hoboken, NJ: Wiley)